

Research Article

Bifurcation Approach to Analysis of Travelling Waves in Nonlocal Hydrodynamic-Type Models

Jianping Shi¹ and Jibin Li²

¹ Department of Mathematics, Kunming University of Science and Technology, Kunming, Yunnan 650093, China

² Department of Mathematics, Zhejiang Normal University, Jinhua, Zhejiang 321004, China

Correspondence should be addressed to Jianping Shi; sjp0207@163.com

Received 7 November 2013; Revised 22 January 2014; Accepted 30 January 2014; Published 18 March 2014

Academic Editor: Wen-Xiu Ma

Copyright © 2014 J. Shi and J. Li. This is an open access article distributed under the Creative Commons Attribution License, which permits unrestricted use, distribution, and reproduction in any medium, provided the original work is properly cited.

The paper considers the nonlocal hydrodynamic-type systems which are two-dimensional travelling wave systems with a five-parameter group. We apply the method of dynamical systems to investigate the bifurcations of phase portraits depending on the parameters of systems and analyze the dynamical behavior of the travelling wave solutions. The existence of peakons, compactons, and periodic cusp wave solutions is discussed. When the parameter n equals 2, namely, let the isochoric Gruneisen coefficient equal 1, some exact analytical solutions such as smooth bright solitary wave solution, smooth and nonsmooth dark solitary wave solution, and periodic wave solutions, as well as uncountably infinitely many breaking wave solutions, are obtained.

1. Introduction

A hydrodynamic system of balance equations for mass and momentum is considered by Vladimirov et al. [1]:

$$\begin{aligned} u_t + p_x &= \frac{\mathfrak{F}}{\rho}, \\ \rho_t + \rho^2 u_x &= 0, \\ \hat{\tau} p_t + p &= \frac{\beta}{\nu + 2} \rho^{\nu+2} + \sigma \left[\rho^{\nu+1} \rho_{xx} + (\nu + 1) \rho^\nu (\rho_x)^2 \right], \end{aligned} \quad (1)$$

where $\nu = n - 2$, $n = 1 + \Gamma_V \infty$, $\Gamma_V \infty$ is the isochoric Gruneisen coefficient [2], and $\hat{\tau}$, β , and σ are parameters. This system is closed by the dynamic equation of state, taking into account the effects of spatiotemporal nonlocalities. Using group theory reduction, the authors of [1] obtained the following system of the ordinary differential equations:

$$\dot{R} = Y,$$

$$\begin{aligned} \sigma R^{\nu+2} \dot{Y} &= GR - \left[D^2 + \frac{\beta}{\nu + 2} R^{\nu+3} + \sigma (\nu + 1) R^{\nu+1} Y^2 \right] - \tau \epsilon \frac{D^3}{R} Y, \\ \dot{G} &= \epsilon \left[f(R) - \xi \left(C_1 + \frac{1 - \nu D}{1 + \nu R} \right) \right], \end{aligned} \quad (2)$$

which describes a set of approximate travelling wave solutions to the source system (1) (see the initial system (1) of PDEs in [1]), where τ , ξ and C_1 , D are constant parameters; $\epsilon \ll 0$.

When $\epsilon = 0$, it immediately obtains that $G = G_1 = \text{const}$, and the system (2) reduces to the following two-dimensional system:

$$\begin{aligned} \frac{dR}{d\zeta} &= Y, \\ \frac{dY}{d\zeta} &= \frac{G_1 R - \left[D^2 + (\beta / (\nu + 2)) R^{\nu+3} + \sigma (\nu + 1) R^{\nu+1} Y^2 \right]}{\sigma R^{\nu+2}}, \end{aligned} \quad (3)$$

where $\zeta = x - Dt$.

Assume that $A_j(R_j, 0)$, $j = 1, 2$, are two equilibrium points of system (3). Vladimirov et al. obtained the following conclusion (see [1, 3]).

Theorem A. *If $\nu > -2$ and $D^2 > \beta R_1^{\nu+3}$, then system (3) possesses a one-parameter family of periodic solutions, localized around the critical point $A_2(R_2, 0)$ in a bounded set M . The boundary of this set is formed by the homoclinic intersection of separatrices of the saddle point $A_1(R_1, 0)$.*

We notice that for a fixed ν , system (3) is a four-parameter system depending on the parameter group (β, σ, D, G_1) . The bifurcations and dynamical behavior of solutions of system (3) have not been studied by [1, 3]. The conclusion of Theorem A is incomplete (see Theorems 1–3 of Section 3 below). In fact, system (3) is the first class of singular travelling wave systems defined by [4, 5], which has the singular straight line $R = 0$. Depending on the changes of parameters, there are very interesting bifurcations and dynamical behaviors of the travelling wave solutions in this kind of singular systems, for example, it gives rise to so-called peakons, compactons, loop solutions, and others. As Fokas stated that peakons are peaked solitons [6], that is, solitons with discontinuous first derivative, compactons are solitons with compact support.

In this paper, we will give complete description for the dynamics of solutions of system (3).

Instead of ν , we use $n = \nu + 2$ to rewrite (3) as follows:

$$\begin{aligned} \frac{dR}{d\zeta} &= Y, \\ \frac{dY}{d\zeta} &= \frac{G_1 R - [D^2 + (\beta/n) R^{n+1} + \sigma(n-1) R^{n-1} Y^2]}{\sigma R^n}. \end{aligned} \tag{4}$$

This system has the first integral:

$$H(R, Y) = Y^2 R^{2n-2} + \frac{2R^{n-1}}{n\sigma} \left[\frac{nD^2}{n-1} - G_1 R + \frac{\beta}{2n} R^{n+1} \right] = h. \tag{5}$$

Clearly, in order to make $H(R, Y)$ well defined, we assume that $n > 1$; that is, $\nu > -1$.

This paper is organized as follows. In Section 2, we analyse the bifurcations of phase portraits of system (4) under different parameter conditions. Section 3 discusses the existence of periodic solutions in different parameter conditions. In particular, it discusses the existence of solitary cusp wave solutions (peakons) and periodic cusp wave solutions. In Section 4, for the case $n = \nu + 2 = 2$, namely, let the isochoric Gruneisen coefficient equal 1, we figure out explicit parametric expressions for the solitary wave solutions, periodic wave solutions, and uncountably infinitely many breaking wave solutions (compactons). Finally, we give a conclusion of this paper.

2. Bifurcations of the Phase Portraits of System (4)

In this section, we study the phase portraits of system (4) in the (R, Y) -phase plane. Consider the associated regular system of (4):

$$\begin{aligned} \frac{dR}{d\eta} &= \sigma R^n Y, \\ \frac{dY}{d\eta} &= G_1 R - \left[D^2 + \frac{\beta}{n} R^{n+1} + \sigma(n-1) R^{n-1} Y^2 \right], \end{aligned} \tag{6}$$

where $d\zeta = \sigma R^n d\eta$. Clearly, now the straight line $R = 0$ is a solution of system (6). On the straight line $R = 0$, system (6) has no equilibrium point.

Consider the following formulas:

$$\begin{aligned} f(R) &= \frac{\beta}{n} R^{n+1} - G_1 R + D^2, \\ f'(R) &= \frac{(n+1)\beta}{n} R^n - G_1. \end{aligned} \tag{7}$$

Obviously, for $n = 2m$, $m = 1, 2, \dots$, when $\beta G_1 > 0$, and $R = R_{M\pm} \equiv \pm(nG_1/(n+1)\beta)^{1/n}$, $f'(R_{M\pm}) = 0$, while for $n = 2m + 1$, $m = 1, 2, \dots$, when $R = R_M \equiv (nG_1/(n+1)\beta)^{1/n}$, $f'(R_M) = 0$; we have $f(R_M) = f(R_{M+}) = f(R_{M-}) = D^2 - (nG_1/(n+1))R_M$. When $D^2 = D_{cr}^2 \equiv (nG_1/(n+1))(nG_1/(n+1)\beta)^{1/n}$, $f(R_M) = 0$.

Since every real root R_j of the function $f(R)$ gives rise to an equilibrium point $A_j(R_j, 0)$ of system (6), by using (7), we can analyse the equilibrium points $A_j(R_j, 0)$ of system (6) in different parameter conditions and have the following conclusions.

2.1. *In the Case of $n = 2m$.* Consider the following.

- (1) For $\beta > 0$ and $G_1 > 0$, when $D^2 < (nG_1/(n+1))R_M$, and $f(R_{M-}) > 0$, $f(R_{M+}) < 0$. There exist three equilibrium points $A_j(R_j, 0)$, $j = 1, 2, 3$, of system (6), satisfying $-\infty < R_1 < R_{M-} < 0 < R_2 < R_{M+} < R_3 < \infty$. When $D^2 = (nG_1/(n+1))R_M$, $f(R_{M-}) > 0$ and $f(R_{M+}) = 0$. There exist two equilibrium points $A_j(R_j, 0)$, $j = 1, 2$, of system (6), satisfying $-\infty < R_1 < R_{M-} < 0 < R_2 = R_{M+} < \infty$. When $D^2 > (nG_1/(n+1))R_M$, $f(R_{M-}) > 0$, and $f(R_{M+}) > 0$. There exists only one equilibrium point $A_1(R_1, 0)$ of system (6), satisfying $-\infty < R_1 < R_{M-} < 0$.
- (2) For $\beta < 0$, and $G_1 < 0$, when $D^2 < (n|G_1|/(n+1))R_M$, $f(R_{M-}) < 0$, and $f(R_{M+}) > 0$. There exist three equilibrium points $A_j(R_j, 0)$, $j = 1, 2, 3$, of system (6), satisfying $-\infty < R_1 < R_{M-} < R_2 < 0 < R_{M+} < R_3 < \infty$. When $D^2 = (n|G_1|/(n+1))R_M$, $f(R_{M-}) = 0$, and $f(R_{M+}) > 0$. There exist two equilibrium points $A_j(R_j, 0)$, $j = 1, 2$, of system (6), satisfying $-\infty < R_1 = R_{M-} < 0 < R_{M+} < R_2 < \infty$. When $D^2 > (n|G_1|/(n+1))R_M$, $f(R_{M-}) > 0$, and $f(R_{M+}) > 0$. There exists only one equilibrium point

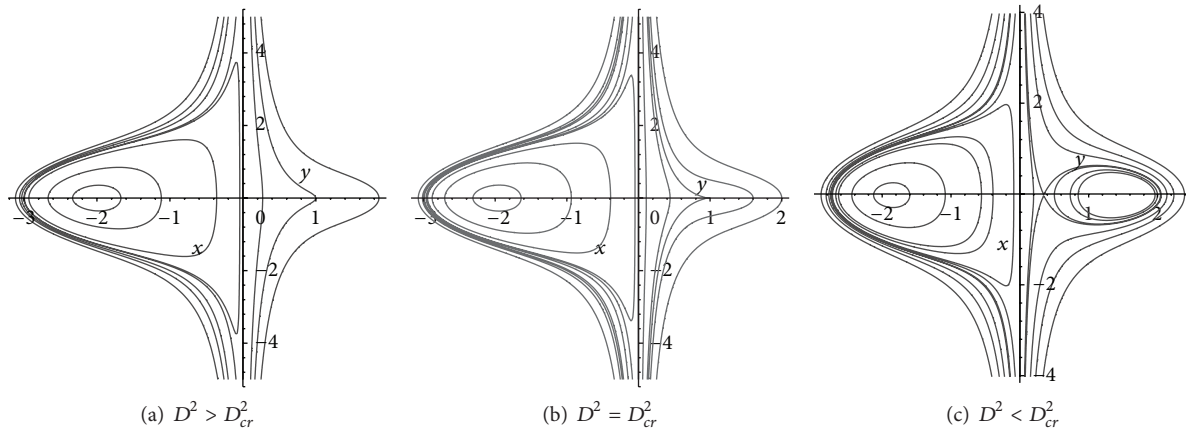


FIGURE 1: The phase portraits of system (6) for $n = 2m, \beta > 0, G_1 > 0,$ and $\sigma > 0.$

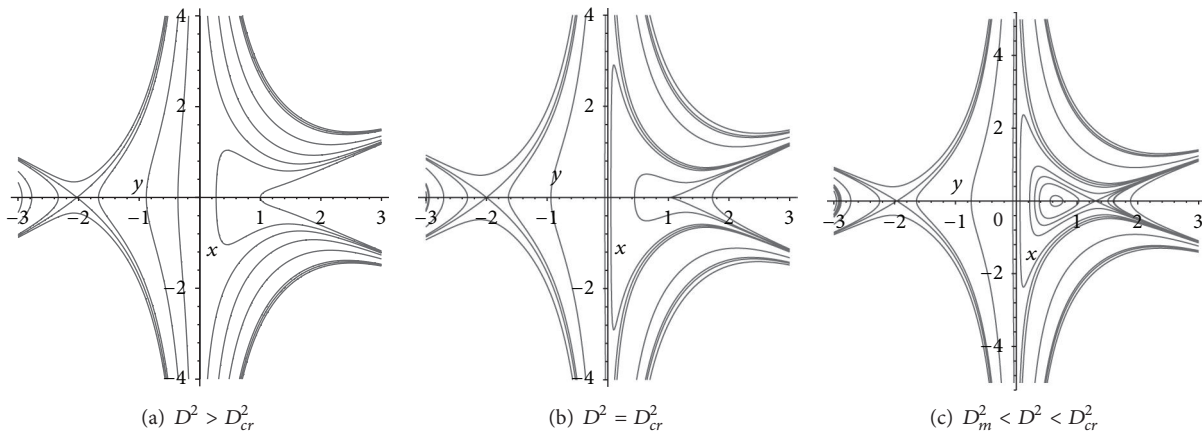


FIGURE 2: The phase portraits of system (6) for $n = 2m, \beta > 0, G_1 > 0,$ and $\sigma < 0.$

- $A_1(R_1, 0)$ of system (6), satisfying $0 < R_{M+} < R_1 < \infty.$
- (3) For $\beta > 0, G_1 < 0,$ and any given $D, \sigma,$ because the number R_M is not real, there exists one equilibrium point $A_1(R_1, 0)$ of system (6), satisfying $-\infty < R_1 < 0.$
- (4) For $\beta < 0, G_1 > 0,$ and any given $D, \sigma,$ there exists one equilibrium point $A_1(R_1, 0)$ of system (6), satisfying $0 < R_1 < \infty.$

Let $M(R_j, 0)$ be the coefficient matrix of the linearized system of system (6) at an equilibrium point $A_j(R_j, 0).$ We have

$$J(R_j, 0) = \det M(R_j, 0) = \sigma R_j^n f'(R_j). \tag{8}$$

By the theory of planar dynamical systems, for an equilibrium point of a planar integrable system, if $J < 0,$ then the equilibrium point is a saddle point; if $J > 0,$ and $(\text{Trace}M(R_j, 0))^2 - 4J(R_j, 0) > 0,$ then it is a node point; if $J > 0,$ and $\text{Trace}M(R_j, 0) = 0,$ then, it is a center point; if $J = 0$ and the Poincaré index of the equilibrium point is 0, then this equilibrium point is cusp [5].

According to formula (5), we write that $h_0 = H(0, 0) = 0$ and $h_j = H(R_j, 0), j = 1, 2, 3.$

By using the above results, we have the following bifurcations of phase portraits of system (6) shown in Figures 1-5.

For the case of $\beta < 0,$ and $G_1 < 0,$ we see from system (6) that when $n = 2m,$ by the transformation $R \rightarrow -R, Y \rightarrow -Y,$ and $\sigma \rightarrow -\sigma,$ it can become the case of $\beta > 0, G_1 > 0.$ Thus, the phase portraits of system (6) in the case of $\beta < 0,$ and $G_1 < 0$ just are the reflections of the phase portraits in Figures 1 and 2 with respect to the Y -axis, which are shown in Figures 3 and 4.

2.2. In the Case of $n = 2m + 1.$ Consider the following.

- (1) For $\beta > 0,$ and $G_1 > 0,$ when $D^2 < (nG_1/(n + 1))R_M,$ and $f(R_M) < 0,$ there exist two equilibrium points $A_j(R_j, 0), j = 1, 2,$ of system (6), satisfying $0 < R_1 < R_M < R_2 < \infty.$ When $D^2 = (nG_1/(n + 1))R_M,$ and $f(R_M) = 0,$ there exists one equilibrium point $A_1(R_1, 0)$ of system (6), satisfying $0 < R_1 = R_M < \infty.$ When $D^2 > (nG_1/(n + 1))R_M,$ and $f(R_M) > 0,$ system (6) has no equilibrium point.

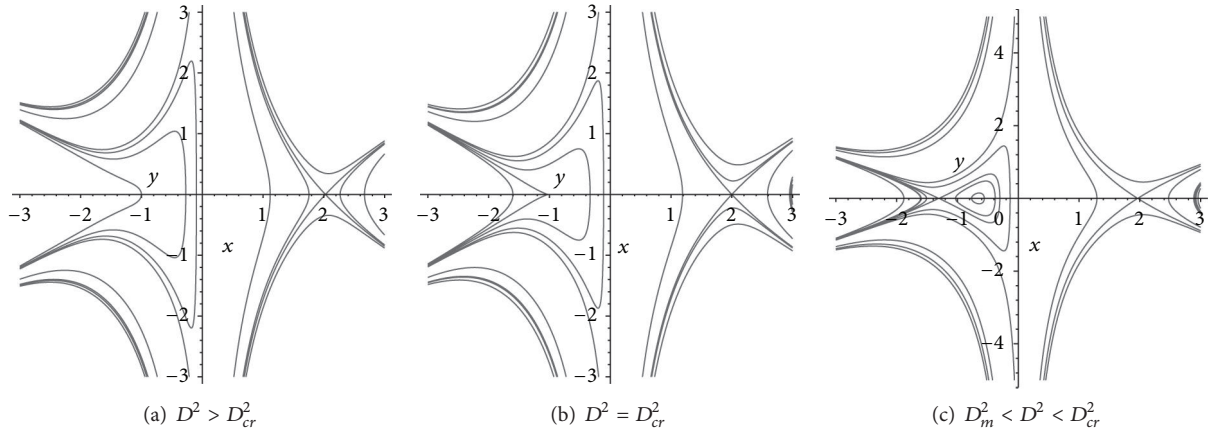


FIGURE 3: The phase portraits of system (6) for $n = 2m$, $\beta < 0$, $G_1 < 0$, and $\sigma > 0$.

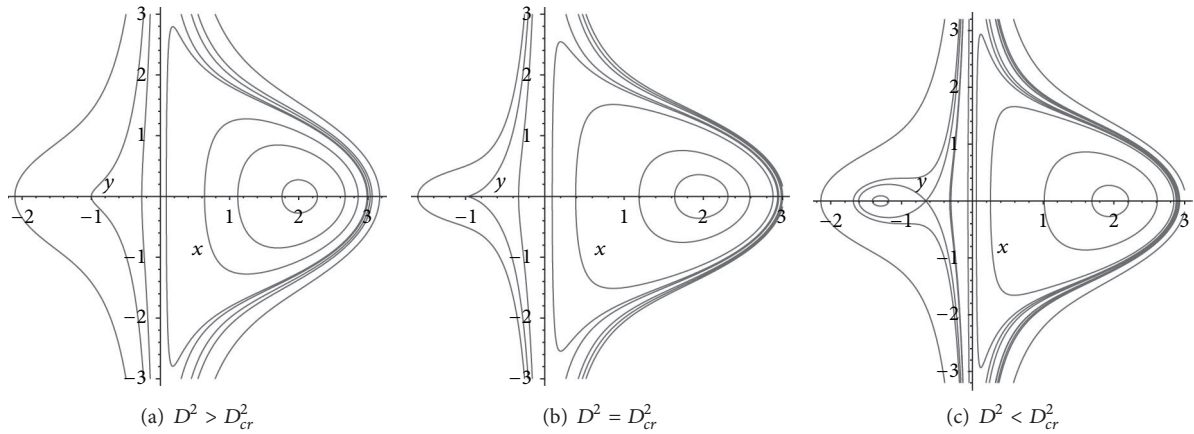


FIGURE 4: The phase portraits of system (6) for $n = 2m$, $\beta < 0$, $G_1 < 0$, and $\sigma < 0$.

- (2) For $\beta > 0$, $G_1 < 0$, when $D^2 < (nG_1/(n + 1))R_M$, and $f(R_M) < 0$, there exist two equilibrium points $A_j(R_j, 0)$, $j = 1, 2$, of system (6), satisfying $-\infty < R_1 < R_M < R_2 < 0$. When $D^2 = (nG_1/(n + 1))R_M$, and $f(R_M) = 0$, there exists one equilibrium point $A_1(R_1, 0)$ of (6), satisfying $-\infty < R_1 = R_M < 0$. When $D^2 > (nG_1/(n + 1))R_M$, and $f(R_M) > 0$, system (6) has no equilibrium point.
- (3) For $\beta < 0$, $G_1 > 0$, and any given D, σ , there exist two equilibrium points $A_j(R_j, 0)$, $j = 1, 2$, of system (6), satisfying $-\infty < R_1 < R_M < 0 < R_2$.
- (4) For $\beta < 0$, $G_1 < 0$, and any given D, σ , there exist two equilibrium points $A_j(R_j, 0)$, $j = 1, 2$, of system (6), satisfying $-\infty < R_1 < 0 < R_M < R_2 < \infty$.

Same as Section 2.1, we have the following bifurcations of phase portraits of system (6) shown in Figures 6–10.

3. The Existence of Solutions of System (4)

Because system (6) has the same phase orbits as system (4), therefore, to sum up, by the above discussion, we have the following results.

3.1. The Existence of Periodic Solutions

Theorem 1. (1) If $\beta > 0$, $G_1 > 0$, $\sigma > 0$, and $D^2 < D_{cr}^2 \equiv (nG_1/(n + 1))(nG_1/(n + 1)\beta)^{1/n}$, then, for any $n = \nu - 2 = 2m > 1$, system (4) possesses a one-parameter family of periodic solutions defined by $H(R, Y) = h$, $h \in (h_3, h_2)$, enclosing the center point $A_3(R_3, 0)$. The boundary of this set is formed by the homoclinic orbit defined by $H(R, Y) = h_2$ to the saddle point $A_2(R_2, 0)$ (see Figure 1(c)).

And for any $n = \nu - 2 = 2m + 1$, system (4) possesses a one-parameter family of periodic solutions defined by $H(R, Y) = h$, $h \in (h_2, h_1)$, enclosing the center point $A_2(R_2, 0)$. The boundary of this set is formed by the homoclinic orbit defined by $H(R, Y) = h_1$ to the saddle point $A_1(R_1, 0)$ (see Figure 6(c)).

(2) If $\beta > 0$, $G_1 > 0$, $\sigma < 0$, and $D_m^2 < D^2 < D_{cr}^2 \equiv (nG_1/(n + 1))(nG_1/(n + 1)\beta)^{1/n}$, then, for any $n = \nu - 2 =$

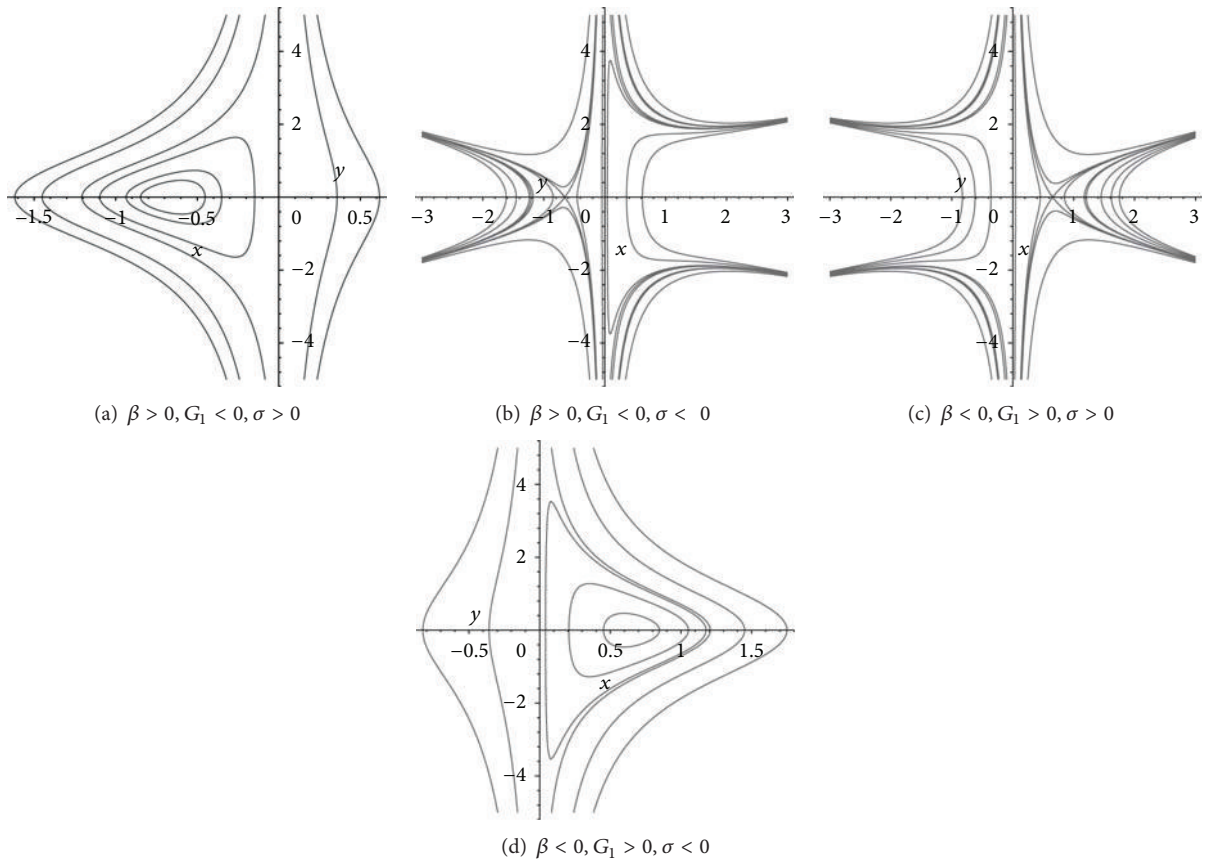


FIGURE 5: The phase portraits of system (6) for $n = 2m$, and $\beta G_1 < 0$.

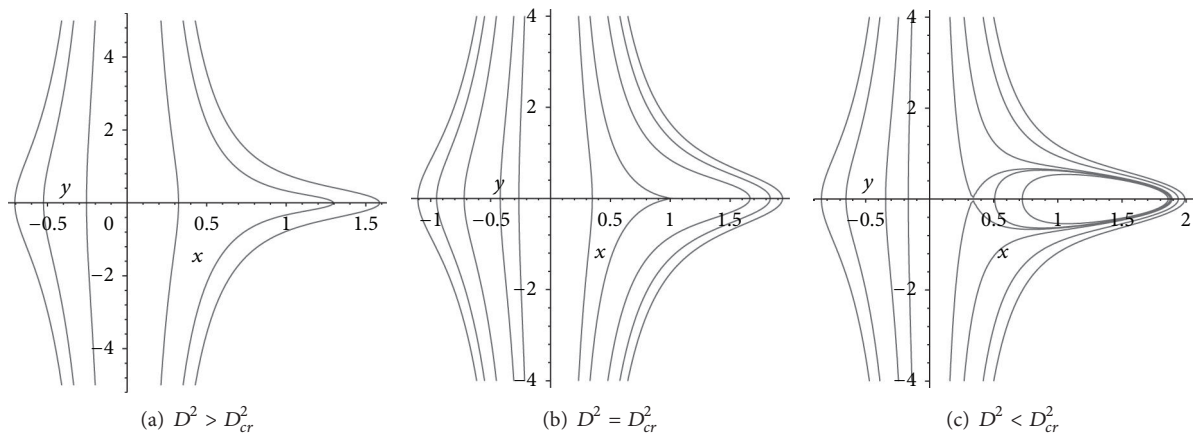


FIGURE 6: The phase portraits of system (6) for $n = 2m + 1, \beta > 0, G_1 > 0$, and $\sigma > 0$.

$2m > 1$, system (4) possesses a one-parameter family of periodic solutions defined by $H(R, Y) = h, h \in (h_2, h_3)$, enclosing the center point $A_2(R_2, 0)$. The boundary of this set is formed by the homoclinic orbit defined by $H(R, Y) = h_3$ to the saddle point $A_3(R_3, 0)$ (see Figure 2(c)).

And for any $n = \nu - 2 = 2m + 1$, system (4) possesses a one-parameter family of periodic solutions defined by $H(R, Y) = h, h \in (h_1, h_2)$, enclosing the center point

$A_1(R_1, 0)$. The boundary of this set is formed by the homoclinic orbit defined by $H(R, Y) = h_2$ to the saddle point $A_2(R_2, 0)$ (see Figure 7(c)).

Theorem 2. (1) If $\beta < 0, G_1 < 0, \sigma < 0$ (or $\beta > 0, G_1 < 0, \sigma > 0$), and $D^2 < D_{cr}^2 \equiv (nG_1/(n+1))(nG_1/(n+1)\beta)^{1/n}$, then, for any $n = \nu - 2 > 1$, system (4) possesses a one-parameter family of periodic solutions defined by $H(R, Y) = h, h \in (h_1, h_2)$,

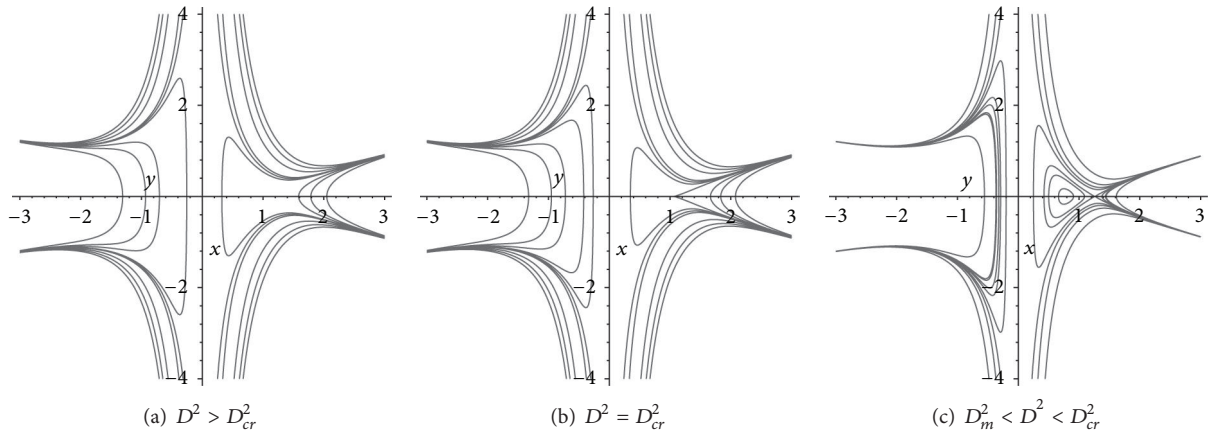


FIGURE 7: The phase portraits of system (6) for $n = 2m + 1$, $\beta > 0$, $G_1 > 0$, and $\sigma < 0$.

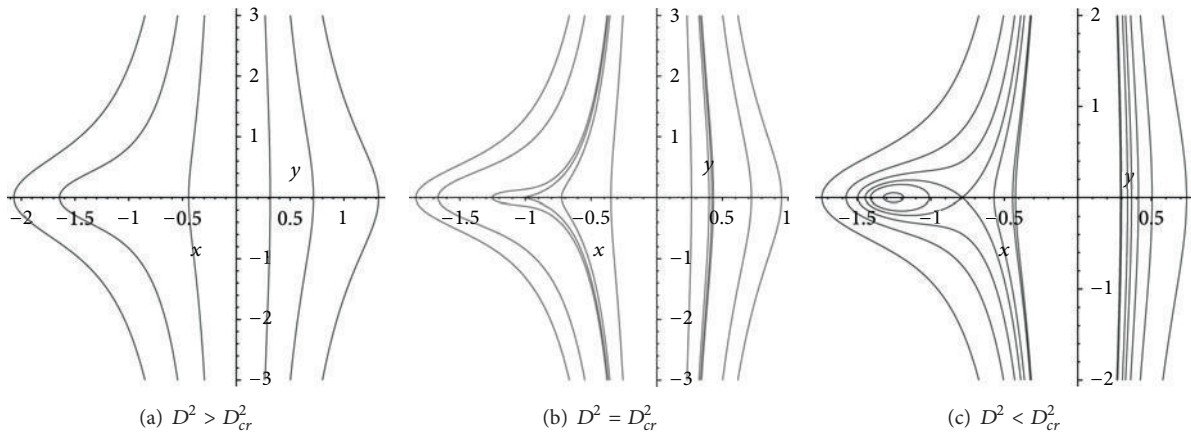


FIGURE 8: The phase portraits of system (6) for $n = 2m + 1$, $\beta > 0$, $G_1 < 0$, and $\sigma > 0$.

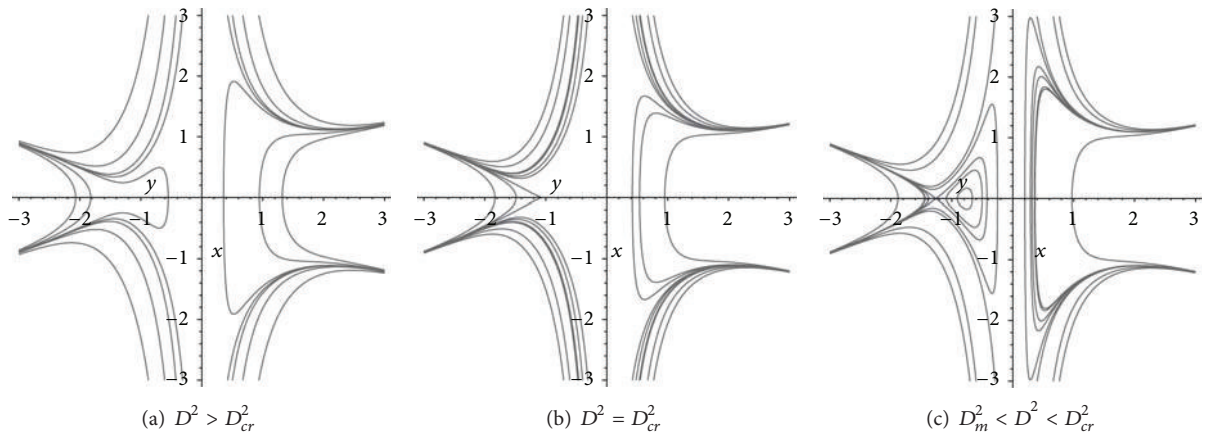


FIGURE 9: The phase portraits of system (6) for $n = 2m + 1$, $\beta > 0$, $G_1 < 0$, and $\sigma < 0$.

enclosing the center point $A_1(R_1, 0)$. The boundary of this set is formed by the homoclinic orbit defined by $H(R, Y) = h_2$ to the saddle point $A_2(R_2, 0)$ (see Figure 4(c) or Figure 8(c)).

(2) If $\beta < 0$, $G_1 < 0$, $\sigma > 0$ (or $\beta > 0$, $G_1 < 0$, $\sigma < 0$), and $D_m^2 < D^2 < D_{cr}^2 \equiv (nG_1/(n + 1))(nG_1/(n + 1)\beta)^{1/n}$, then, for

any $n = \nu - 2 > 1$, system (4) possesses a one-parameter family of periodic solutions defined by $H(R, Y) = h$, $h \in (h_2, h_1)$, enclosing the center point $A_2(R_2, 0)$. The boundary of this set is formed by the homoclinic orbit defined by $H(R, Y) = h_1$ to the saddle point $A_1(R_1, 0)$ (see Figure 3(c) or Figure 9(c)).

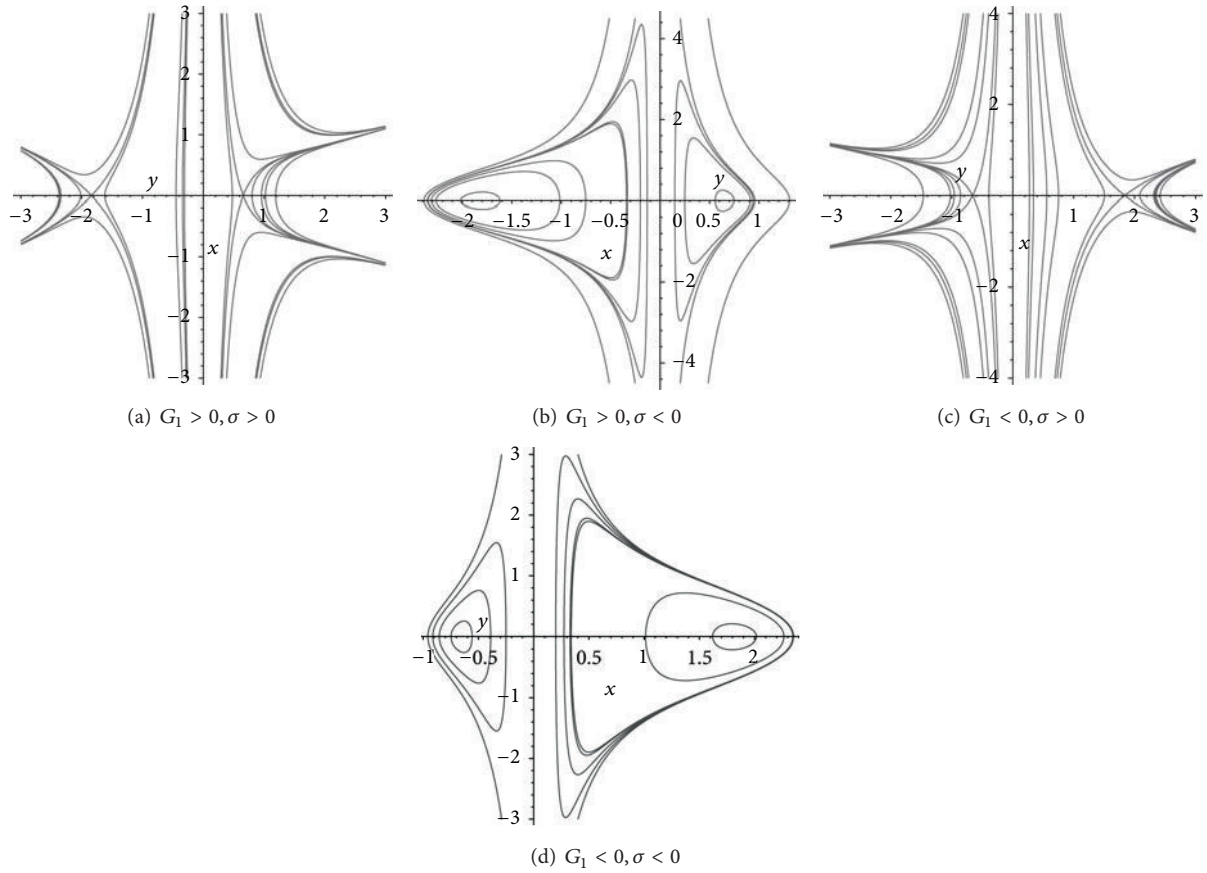


FIGURE 10: The phase portraits of system (6) for $n = 2m + 1$, and $\beta < 0$.

Theorem 3. (1) If one of the following conditions holds:

- (a) $\beta > 0, G_1 > 0, \sigma > 0$;
- (b) $\beta < 0, G_1 < 0, \sigma < 0$;
- (c) $\beta > 0, G_1 < 0, \sigma > 0$;
- (d) $\beta < 0, G_1 > 0, \sigma < 0$,

then, for any $n = 2m > 1$ and $D^2 > 0$, system (4) possesses a one-parameter family of periodic solutions defined by $H(R, Y) = h, h \in (h_j, 0)$, enclosing the center point $A_j(R_j, 0)$ (see Figures 1, 4, and 5(a), 5(d)). As $h \rightarrow 0$, the closed orbits of system (4) expand outwards and approach to the singular straight line $R = 0$.

(2) If one of the following conditions holds:

- (a) $\beta < 0, G_1 > 0, \sigma < 0$;
- (b) $\beta < 0, G_1 < 0, \sigma < 0$,

then, for any $n = 2m + 1$ and $D^2 > 0$, system (4) possesses two families of periodic solutions defined by $H(R, Y) = h, h \in (h_j, 0), j = 1, 2$, enclosing the center point $A_j(R_j, 0), j = 1, 2$ (see Figures 10(b) and 10(d)). As $h \rightarrow 0$, the closed orbits of system (4) expand outwards and approach to the singular straight line $R = 0$.

3.2. *The Existence of Uncountably Infinitely Periodic Cusp Wave Solutions and Pseudo-Peakons.* We consider Figure 3(c), for every fixed n, β, σ , and G_1 , when parameter D^2 decreases from D_{cr}^2 to 0, there exists a value $D^2 = D_m^2$ (where D_m^2 satisfies $H(R_1, 0) = h_1 = 0$) such that when $D^2 < D_m^2$, the stable and unstable manifolds to a saddle point cannot connect in R -axis. Corresponding to Figure 3(c), the changes of phase portraits of system (6) are shown in Figure 11. For a fixed parameter group of n, β, G_1 , and σ , the value of D_m^2 can be numerically determined.

We see from Section 2 that if $n = 2m$, when $\beta > 0, G_1 > 0, \sigma < 0$, and $D_m < D^2 < D_{cr}^2$, system (4) has the phase portrait Figure 2(c), while when $\beta < 0, G_1 < 0, \sigma > 0$, and $D_m < D^2 < D_{cr}^2$, system (4) has the phase portrait Figure 3(c). Similarly, if $n = 2m + 1$, when $\beta > 0, G_1 > 0, \sigma < 0$, and $D_m < D^2 < D_{cr}^2$, system (4) has the phase portrait Figure 7(c), while when $\beta > 0, G_1 < 0, \sigma < 0$ and $D_m < D^2 < D_{cr}^2$, system (4) has the phase portrait Figure 9(c).

According to all the above, for a fixed parameter group (n, β, G_1, σ) , when parameter D^2 decreases from D_{cr}^2 to D_m , the homoclinic orbit loop will gradually expand and approach to the straight line $R = 0$ (see Figure 11). By using the rapid-jump property of $dR/d\zeta$ near the straight line given by [4], it implies that depending on $D^2 \in (D_m^2, D_{cr}^2)$,

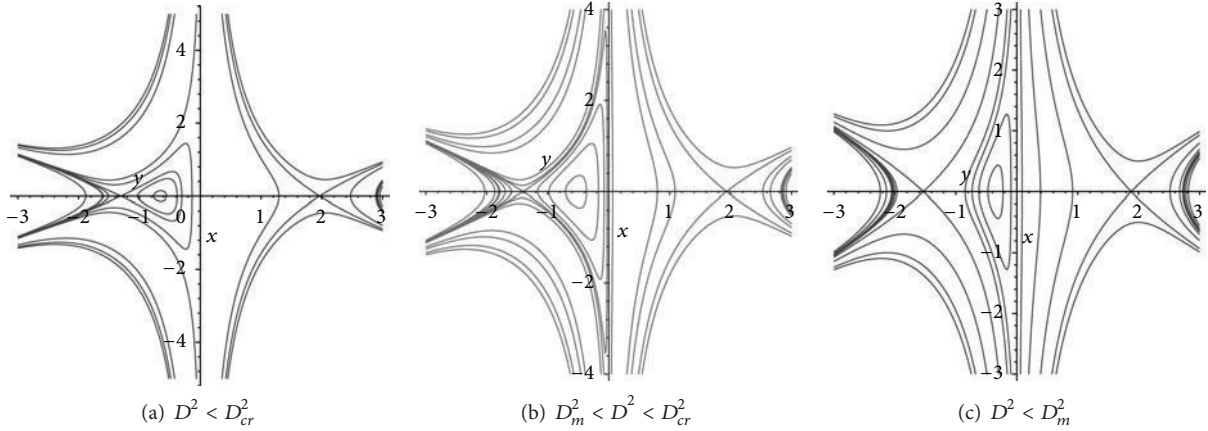


FIGURE 11: The changes of phase portraits of system (6) when D^2 are decreased. Parameters: $n = 2m, \beta < 0, G_1 < 0,$ and $\sigma > 0$.

there exists a family of solitary cusp wave solutions (peaks) of (1). For example, corresponding to the homoclinic orbit in Figure 11(b), we have the peakon shown in Figure 12(a). Corresponding to the periodic orbits defined by $H(R, Y) = h, h \in (h_2, h_1)$ in Figure 11(b), when h is varied from h_2 to h_1 , the periodic wave solutions gradually lose their smoothness, from smooth periodic waves become periodic cusp waves (see Figures 12(b)–12(d)).

Hence, we have the following conclusion.

Theorem 4. Under the above mentioned parameter conditions of Figure 2(c), Figure 3(c), Figure 7(c), and Figure 8(c), for a fixed parameter group (n, β, G_1, σ) , depending on the parameter D^2 , closing to the value D_m , there exist solitary cusp wave solutions (pseudo-peakons) and periodic cusp wave solutions of (1).

4. Analytical Travelling Wave Solutions for $n = 2$

According to (5), for a fixed integral constant h , we have

$$y = \frac{1}{R^{n-1}} \left(h - \frac{2R^{n-1}}{n\sigma} \left[\frac{nD^2}{n-1} - G_1R + \frac{\beta}{2n}R^{n+1} \right] \right)^{1/2}. \quad (9)$$

Using the first equation of (4) and taking integration on a branch of the invariant curve $H(R, Y) = h$ with initial value $R(\zeta_0) = R_0$, we have

$$\begin{aligned} & \zeta - \zeta_0 \\ &= \int_{R_0}^R \frac{R^{n-1} dR}{\sqrt{F(R)}} \\ &\equiv \int_{R_0}^R \frac{R^{n-1} dR}{\sqrt{h - (2R^{n-1}/n\sigma) [nD^2/(n-1) - G_1R + (\beta/2n)R^{n+1}]} }. \end{aligned} \quad (10)$$

In general, for $n \geq 3$, the right side of (10) cannot be integrated explicitly. However, for $n = 2$, introducing a new

parametric variable χ , we can obtain analytical parametric representations for solitary wave solutions, breaking wave solutions and periodic wave solutions of (4).

4.1. In the Case $\beta > 0, G_1 > 0,$ and $\sigma > 0$. Suppose that $D^2 < D_{cr}^2 \equiv (2G_1/3)(2G_1/3\beta)^{1/2}$ (see Figure 1(c)).

(1) Corresponding to the homoclinic orbit to the saddle point $A_2(R_2, 0)$, as a closed branch of the level set $H(R, Y) = h_2$, enclosing the center $A_3(R_3, 0)$ in Figure 1(c), it gives rise to a bright solitary wave solution of (1). Now, we have $F(R) = (1/2)\sqrt{\beta/\sigma}(R_m - R)(R - R_2)^2(R - R_l)$ with $R_l < 0 < R_2 < R_3 < R_m$. Thus, (10) has the following form:

$$\begin{aligned} \frac{1}{2} \sqrt{\frac{\beta}{\sigma}} \zeta &= \int_{R_m}^R \frac{R dR}{(R - R_2) \sqrt{(R_m - R)(R - R_l)}} \\ &= \int_{R_m}^R \left[\frac{1}{\sqrt{(R_m - R)(R - R_l)}} \right. \\ &\quad \left. + \frac{R_2}{(R - R_2) \sqrt{(R_m - R)(R - R_l)}} \right] dR. \end{aligned} \quad (11)$$

The following analytical parametric representation of the bright solitary wave solution of (1) can be obtained:

$$\begin{aligned} R(\chi) &= R_2 + \frac{2(R_m - R_2)(R_2 - R_l)}{(R_m - R_l) \cosh(\omega\zeta) - (R_m - 2R_2 + R_l)}, \\ \zeta(\chi) &= 2\sqrt{\frac{\sigma}{\beta}} \left[R_2\chi - \frac{\pi}{2} - \arcsin\left(\frac{R_m + R_l - 2R(\chi)}{R_m - R_l}\right) \right], \end{aligned}$$

for $\chi \in (-\infty, 0]$,

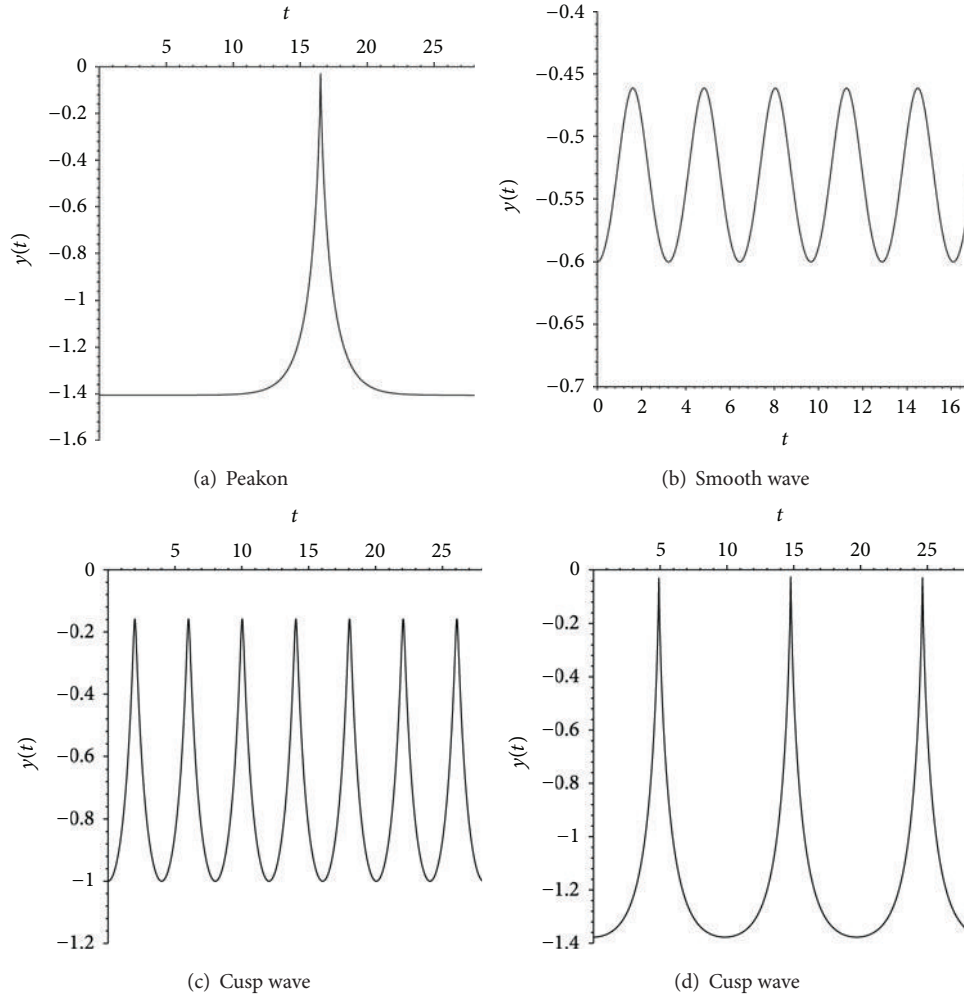


FIGURE 12: The profiles of pseudo-peakon and periodic cusp wave solutions of (1).

$$\zeta(\chi) = 2\sqrt{\frac{\sigma}{\beta}} \left[R_2\chi + \frac{\pi}{2} + \arcsin\left(\frac{R_m + R_l - 2R(\chi)}{R_m - R_l}\right) \right],$$

for $\chi \in [0, \infty)$,

(12)

$$= \int_{r_2}^R \left[\sqrt{\frac{R - r_3}{(r_1 - R)(R - r_2)(R - r_4)}} + \frac{r_3}{\sqrt{(r_1 - R)(R - r_2)(R - r_3)(R - r_4)}} \right] dR.$$

(13)

where $\omega = \sqrt{(R_m - R_2)(R_2 - R_l)}$.

(2) Corresponding to the periodic orbits defined by $H(R, Y) = h$, $h \in (h_3, h_2)$, enclosing the center $A_3(R_3, 0)$ in Figure 1(c), we have a family of periodic wave solutions of (1). Now, $F(R) = (1/2)\sqrt{\beta/\sigma}(r_1 - R)(R - r_2)(R - r_3)(R - r_4)$ with $r_4 < 0 < r_3 < R_2 < r_2 < R_3 < r_1 < R_m$.

Hence, (10) gives that

$$\frac{1}{2}\sqrt{\frac{\beta}{\sigma}}\zeta = \int_{r_2}^R \frac{R dR}{\sqrt{(r_1 - R)(R - r_2)(R - r_3)(R - r_4)}}$$

It implies the following analytical parametric representation of periodic wave solutions of (1):

$$R(\chi) = r_3 + \frac{r_2 - r_3}{1 - \alpha^2 \text{sn}^2(\chi, k)},$$

$$\zeta(\chi) = 2\sqrt{\frac{\sigma}{\beta}} \left[r_3 g\chi + (r_2 - r_3) \Pi(\arcsin(\text{sn}(\chi, k)), \alpha^2, k) \right],$$

(14)

where $g = 2/\sqrt{(r_1 - r_3)(r_2 - r_4)}$, $\alpha^2 = (r_1 - r_2)/(r_1 - r_3)$, $k^2 = (r_1 - r_2)(r_3 - r_4)/(r_1 - r_3)(r_2 - r_4)$ and $\Pi(\cdot, \alpha^2, k)$ is the elliptic integral of the third kind, $\text{sn}(u, k)$ is the Jacobian elliptic function (see [7]).

(3) Corresponding to two families of the periodic orbits defined by $H(R, Y) = h, h \in (h_1, h_3), h_1 < h_3 < 0 < h_2$ enclosing the center $A_1(R_1, 0)$ and $A_3(R_3, 0)$, respectively, in Figure 1(c), we have $F(R) = (1/2)\sqrt{\beta/\sigma}(r_1 - R)(R - r_2)(R - r_3)(R - r_4)$ and $F(R) = (1/2)\sqrt{\beta/\sigma}(r_1 - R)(r_2 - R)(r_3 - R)(R - r_4)$, respectively, with $r_4 < R_1 < r_3 < 0 < R_2 < r_2 < R_3 < r_1 < R_m$. In this case, the right family of the periodic orbits has the same parametric representation as (14). For the left family of periodic orbits, formula (10) has the following form:

$$\begin{aligned} & \frac{1}{2} \sqrt{\frac{\beta}{\sigma}} \zeta \\ &= \int_R^{r_3} \frac{R dR}{\sqrt{(r_1 - R)(r_2 - R)(r_3 - R)(R - r_4)}} \\ &= \int_R^{r_3} \left[-\sqrt{\frac{r_2 - R}{(r_1 - R)(r_3 - R)(R - r_4)}} \right. \\ & \quad \left. + \frac{r_2}{\sqrt{(r_1 - R)(r_2 - R)(r_3 - R)(R - r_4)}} \right] dR. \end{aligned} \tag{15}$$

It implies the following analytical parametric representation of the left family of periodic wave solutions of (1):

$$R(\chi) = r_3 - \frac{\alpha_1^2 (r_2 - r_3) \text{sn}^2(\chi, k)}{1 - \alpha_1^2 \text{sn}^2(\chi, k)},$$

$$\begin{aligned} & \zeta(\chi) \\ &= 2\sqrt{\frac{\sigma}{\beta}} \left[r_2 g \chi - (r_2 - r_3) \Pi(\arcsin(\text{sn}^2(\chi, k)), \alpha_1^2, k) \right], \end{aligned} \tag{16}$$

where $g = 2/\sqrt{(r_1 - r_3)(r_2 - r_4)}$, $\alpha_1^2 = (r_3 - r_4)/(r_2 - r_4)$, $k^2 = (r_1 - r_2)(r_3 - r_4)/(r_1 - r_3)(r_2 - r_4)$.

(4) Corresponding to two families of open level curves defined by $H(R, Y) = h, h \in (0, h_2), h_2 > 0$ in the two sides of the straight line $R = 0$ in Figure 1(c) (see also Figure 13(a)), we have $F(R) = (1/2)\sqrt{\beta/\sigma}(r_1 - R)(r_2 - R)(r_3 - R)(R - r_4)$ with $r_4 < R_1 < r_3 < 0 < R_2 < r_2 < R_3 < r_1 < R_m$. Thus, the left family of open level curves has the same parametric representation as (16) with $-\chi_0 < \chi < \chi_0, \chi_0 = \text{sn}^{-1}(\sqrt{r_3/\alpha_1^2 r_2}, k)$.

Figures 13(b) and 13(c) show the two families of uncountably infinitely many breaking wave solutions (compactons) of (1).

4.2. In the Case $\beta > 0, G_1 > 0, \sigma < 0$. Suppose that $D_m < D^2 < D_{cr}^2 \equiv (2G_1/3)(2G_1/3\beta)^{1/2}$ (see Figure 2(c)).

(1) Corresponding to the homoclinic orbit to the saddle point $A_3(R_3, 0)$, as a closed branch of the level set $H(R, Y) = h_2$, enclosing the center $A_2(R_2, 0)$ in Figure 2(c), it gives rise to a dark solitary wave solution of (1). In this case, we have $F(R) = (1/2)\sqrt{\beta/|\sigma|}(R_3 - R)^2(R - R_m)(R - R_l)$ with $R_l < 0 < R_m < R_2 < R_3$. Thus, formula (10) has the following form:

$$\begin{aligned} & \frac{1}{2} \sqrt{\frac{\beta}{|\sigma|}} \zeta \\ &= \int_{R_m}^R \frac{R dR}{(R_3 - R) \sqrt{(R - R_m)(R - R_l)}} \\ &= \int_{R_m}^R \left[-\frac{1}{\sqrt{(R - R_m)(R - R_l)}} \right. \\ & \quad \left. + \frac{R_3}{(R_3 - R) \sqrt{(R - R_m)(R - R_l)}} \right] dR. \end{aligned} \tag{17}$$

It implies the following analytical parametric representation of the dark solitary wave solution of (1):

$$\begin{aligned} & R(\chi) \\ &= R_3 - \frac{2(R_3 - R_m)(R_3 - R_l)}{(R_m - R_l) \cosh(\omega_1 \zeta) + (2R_3 - R_m - R_l)}, \\ & \quad \text{for } \chi \in (-\infty, 0], \chi \in [0, \infty), \text{ respectively,} \\ & \zeta(\chi) \\ &= 2\sqrt{\frac{|\sigma|}{\beta}} \left[R_3 \chi \mp \left(\ln \left(\frac{R_m - R_l}{2} \right) \right. \right. \\ & \quad \left. \left. - \ln \left(\sqrt{(R(\chi) - R_m)(R(\chi) - R_l)} \right. \right. \right. \\ & \quad \left. \left. \left. + R(\chi) - \frac{R_m + R_l}{2} \right) \right) \right]. \end{aligned} \tag{18}$$

(2) Corresponding to the periodic orbits defined by $H(R, Y) = h, h \in (h_2, h_3)$, enclosing the center $A_2(R_2, 0)$ in Figure 2(c), we have a family of periodic wave solutions of (1). Now, $F(R) = (1/2)\sqrt{\beta/|\sigma|}(r_1 - R)(r_2 - R)(R - r_3)(R - r_4)$ with $r_4 < 0 < r_3 < R_2 < r_2 < R_3 < r_1$.

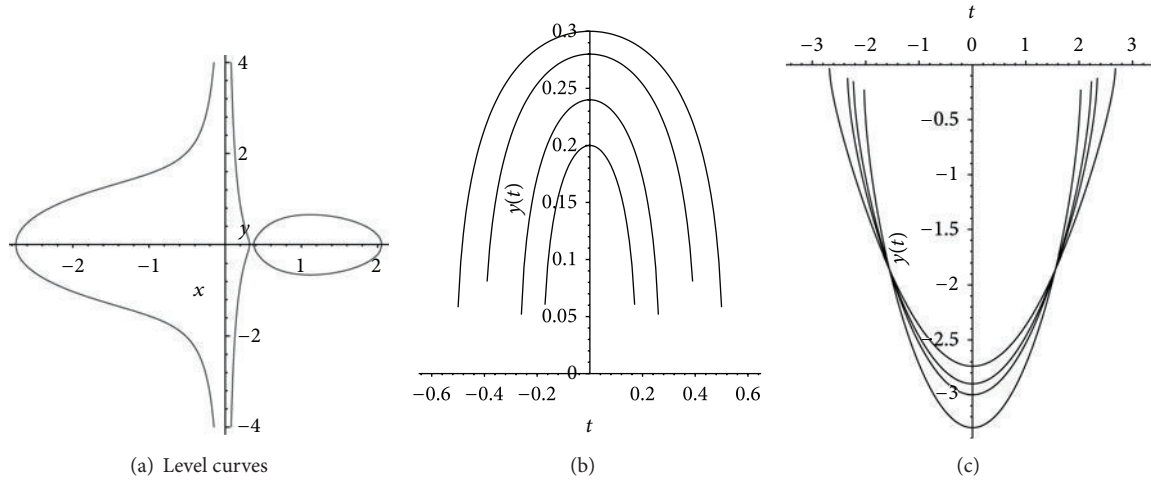


FIGURE 13: The level curves and profiles of breaking wave solutions of (1).

Hence, (10) gives that

$$\begin{aligned}
 & \frac{1}{2} \sqrt{\frac{\beta}{\sigma}} \zeta \\
 &= \int_{r_3}^R \frac{R dR}{\sqrt{(r_1 - R)(r_2 - R)(R - r_3)(R - r_4)}} \\
 &= \int_{r_3}^R \left[\frac{\sqrt{R - r_4}}{\sqrt{(r_1 - R)(r_2 - R)(R - r_3)}} \right. \\
 & \quad \left. + \frac{r_4}{\sqrt{(r_1 - R)(r_2 - R)(R - r_3)(R - r_4)}} \right] dR.
 \end{aligned}
 \tag{19}$$

It implies the following analytical parametric representation of periodic wave solutions of (1):

$$R(\chi) = r_3 + \frac{\alpha_2^2 (r_3 - r_4) \operatorname{sn}^2(\chi, k)}{1 - \alpha_2^2 \operatorname{sn}^2(\chi, k)},$$

$$\begin{aligned}
 & \zeta(\chi) \\
 &= 2 \sqrt{\frac{|\sigma|}{\beta}} \left[r_4 g \chi + (r_3 - r_4) \Pi(\arcsin(\operatorname{sn}(\chi, k)), \alpha_2^2, k) \right],
 \end{aligned}
 \tag{20}$$

where $g = 2/\sqrt{(r_1 - r_3)(r_2 - r_4)}$, $\alpha_2^2 = (r_2 - r_3)/(r_2 - r_4)$, $k^2 = (r_2 - r_3)(r_1 - r_4)/(r_1 - r_3)(r_2 - r_4)$.

Notice that for a given parameter group of (β, G_1, σ) , when D^2 is close to D_m^2 value, (18) and (20) give rise to solitary cusp wave solution (antipeakon) and periodic cusp wave solutions (see Section 3), respectively.

5. Conclusion

In this paper, we use the method of dynamical systems to investigate the bifurcations of phase portraits of nonlocal hydrodynamic-type models. Depending on the different parameters conditions of the systems, the existence of various travelling wave solutions is discussed. Specially, for $n = 2$, namely, let the isochoric Gruneisen coefficient equal 1, some analytical parametric representations of solutions such as smooth bright solitary, smooth and nonsmooth dark solitary wave, and periodic wave solutions, as well as uncountably infinitely many breaking wave solutions are obtained. These results develop and complete the corresponding studies for the nonlocal hydrodynamic-type models.

Conflict of Interests

The authors declare that there is no conflict of interests regarding the publication of this paper.

Acknowledgments

This work was supported by the National Natural Science Foundation of China (10831003). The authors thank the anonymous reviewers for their valuable comments.

References

- [1] V. A. Vladimirov, E. V. Kutafina, and B. Zorychta, "On the non-local hydrodynamic-type system and its soliton-like solutions," *Journal of Physics A*, vol. 45, no. 8, Article ID 085210, 2012.
- [2] V. M. Sidorets and V. A. Vladimirov, "On the peculiarities of stochastic invariant solutions of a hydrodynamic system accounting for non-local effects," in *Proceedings of the 2nd International Conference on Symmetry in Nonlinear Mathematical Physics*, M. I. Shkil, A. G. Nikitin, and V. M. Boyko, Eds., pp. 409–417, Institute of Mathematics, Kyiv, Ukraine, 1997.
- [3] V. A. Vladimirov and E. V. Kutafina, "On the localized invariant solutions of some non-local hydrodynamic-type models," in

Proceedings of Institute of Mathematics of NAS of Ukraine, A. G. Nikitin, V. M. Boyko, R. O. Popovych, and I. A. Yehorchenko, Eds., vol. 50, pp. 1510–1517, Institute of Mathematics, Kyiv, Ukraine, 2004.

- [4] J. Li and G. Chen, “On a class of singular nonlinear traveling wave equations,” *International Journal of Bifurcation and Chaos in Applied Sciences and Engineering*, vol. 17, no. 11, pp. 4049–4065, 2007.
- [5] J. Li and H. H. Dai, *On the Study of Singular Nonlinear Traveling Wave Equations: Dynamical System Approach*, Science Press, Beijing, China, 2007.
- [6] A. S. Fokas, “On a class of physically important integrable equations,” *Physica D*, vol. 87, no. 1–4, pp. 145–150, 1995.
- [7] P. F. Byrd and M. D. Fridman, *Handbook of Elliptic Integrals for Engineers and Scientists*, Springer, Berlin, Germany, 1971.